



HAL
open science

Beckwith Wiedemann syndrome and Uniparental Disomy 11p: Fine mapping of the recombination breakpoints and evaluation of several techniques.

Pablo Lapunzina, Valeria Romanelli, Heloisa Meneses, Luis Fernández, Victor Martínez-Glez, Ricardo Gracia-Bouthelier, Mario Fraga, Encarna Guillén-Navarro, Julián Nevado, Esther Gean, et al.

► **To cite this version:**

Pablo Lapunzina, Valeria Romanelli, Heloisa Meneses, Luis Fernández, Victor Martínez-Glez, et al.. Beckwith Wiedemann syndrome and Uniparental Disomy 11p: Fine mapping of the recombination breakpoints and evaluation of several techniques.. *European Journal of Human Genetics*, 2011, 10.1038/ejhg.2010.236 . hal-00609411

HAL Id: hal-00609411

<https://hal.science/hal-00609411>

Submitted on 19 Jul 2011

HAL is a multi-disciplinary open access archive for the deposit and dissemination of scientific research documents, whether they are published or not. The documents may come from teaching and research institutions in France or abroad, or from public or private research centers.

L'archive ouverte pluridisciplinaire **HAL**, est destinée au dépôt et à la diffusion de documents scientifiques de niveau recherche, publiés ou non, émanant des établissements d'enseignement et de recherche français ou étrangers, des laboratoires publics ou privés.

Beckwith Wiedemann syndrome and Uniparental Disomy 11p: Fine mapping of the recombination breakpoints and evaluation of several techniques.

Valeria Romanelli^{1,2}, Heloisa N. M. Meneses^{1,2,3}, Luis Fernández^{1,2}, Victor Martínez-Glez^{1,2}, Ricardo Gracia-Bouthelier^{4,5}, Mario Fraga⁶, Encarna Guillén⁷, Julián Nevado^{1,2}, Esther Gean⁸, Loreto Martorell⁸, Victoria Esteban Marfil⁹, Sixto García-Miñaur^{1,2}, Pablo Lapunzina^{1,2,5}.

(1) INGEMM, Instituto de Genética Médica y Molecular, Hospital Universitario La Paz, Universidad Autónoma de Madrid, Spain.

(2) CIBERER, Centro de Investigación Biomédica en Red de Enfermedades Raras, Madrid, Spain.

(3) Estudo Colaborativo Latino Americano de Malformações Congênicas: ECLAMC at Departamento de Genética, Universidade Federal do Rio de Janeiro, Rio de Janeiro, Brazil.

(4) Servicio de Endocrinología Infantil, Hospital Universitario La Paz, Universidad Autónoma de Madrid, Spain.

(5) RESSC, Registro Español de Síndromes de Sobrecrecimiento, Madrid, Spain.

(6) Centro Nacional de Biotecnología (CNB-CSIC), Universidad Autónoma de Madrid, Spain.

(7) Unidad de Genética Clínica, Hospital Virgen de la Arrixaca, Murcia, Spain.

(8) Sección de Genética Molecular, Hospital Sant Joan de Déu, Barcelona, Spain.

(9) Servicio de Pediatría, Hospital de Jaén, Jaén, Spain.

KEYWORDS: Beckwith-Wiedemann syndrome, uniparental disomy, breakpoint, SNP-array.

RUNNING TITLE: BWS and paternal uniparental disomy.

Address for correspondence:

Pablo Lapunzina

INGEMM- Instituto de Genética Médica y Molecular

Hospital Universitario La Paz

Paseo de la Castellana 261

28046- Madrid- Spain

Phone: +34 91 727 7217

Fax: +34 91 207 1040

plapunzina.hulp@salud.madrid.org

Conflict of Interest: The authors declare no conflict of interest.

ABSTRACT

Beckwith-Wiedemann syndrome (BWS) is a phenotypically and genotypically heterogeneous overgrowth syndrome characterized by somatic overgrowth, macroglossia and abdominal wall defects. Other usual findings are hemihyperplasia, embryonal tumors, adrenocortical cytomegaly, ear anomalies, visceromegaly, renal abnormalities, neonatal hypoglycaemia, cleft palate, polydactyly and a positive family history.

BWS is a complex, multigenic disorder associated, in up to 90% of patients, with alteration in the expression or function of one or more genes in the 11p15.5 imprinted gene cluster. There are several molecular anomalies associated with BWS and the large proportion of cases, about 85%, is sporadic and karyotypically normal. One of the mayor categories of BWS molecular alteration (10-20% of cases) is represented by mosaic paternal uniparental disomy (pUPD11), namely patients with two paternally derived copies of chromosome 11p15 and no maternal contribution for that. In these patients, in addition to the effects of *IGF2* overexpression, a decreased level of the maternally expressed gene *CDKN1C* may contribute to the BWS phenotype.

In this paper, we reviewed a series of 9 patients with BWS due to pUPD11 using several methods with the aim to evaluate the percentage of mosaicism, the methylation status at both loci, the extension of the pUPD11 at the short arm and the breakpoints of recombination. Fine mapping of mitotic recombination breakpoints by SNP-array in individuals with UPD and fine estimation of epigenetic defects will provide a basis for understanding the aetiology of BWS, allowing more accurate prognostic predictions and facilitating management and surveillance of individuals with this disorder.

INTRODUCTION

Beckwith-Wiedemann syndrome [BWS (MIM 130650)] is a phenotypically and genotypically heterogeneous overgrowth syndrome characterized by somatic overgrowth, macroglossia and abdominal wall defects. Other usual findings are hemihyperplasia, embryonal tumors, adrenocortical cytomegaly, ear anomalies, visceromegaly, renal abnormalities, neonatal hypoglycaemia, cleft palate, polydactyly and a positive family history¹⁻⁴.

BWS is a complex, multigenic disorder associated, in up to 90% of patients, with alteration in the expression or function of one or more genes in the 11p15.5 imprinted gene cluster⁵ (Figure 1a). There are several molecular anomalies associated with BWS and the large proportion of cases, about 85%, is sporadic and karyotypically normal.

Chromosomal rearrangements are relatively rare (~2-3% of cases) and comprise translocations or inversions (typically maternally inherited), microdeletions of KvDMR⁶ or H19DMR⁷ (maternally inherited) and paternal duplications. Point mutations in *CDKN1C*, a cyclin-dependent kinase inhibitor acting as negative regulator of cell proliferation, have been found in 5-7% of sporadic BWS cases⁸⁻¹¹ and in approximately 40% of cases with a positive family history¹².

The largest molecular subgroup, about 60% of cases, is represented by BWS patients that carry an epigenetic error on one or more members of 11p15.5 imprinted gene cluster. Two main epigenetic alterations in BWS patients have been described, one is represented by gain of methylation at the paternal H19DMR (observed in 5-10% of cases), and it is associated with loss of *H19* expression and *IGF2* biallelic expression^{13,14}. The other alteration is loss of maternal methylation of KvDMR (observed in ~50% of BWS patients), usually accompanied by biallelic expression of the *KCNQ1OT1* transcript and down-regulation of *CDKN1C*¹⁵⁻¹⁷. Finally, another large category of BWS molecular alteration, 10-20% of cases, is represented by paternal uniparental disomy (pUPD), namely patients with two paternally derived copies of chromosome 11p15 and

no maternal contribution for that region^{18,19}. In these patients, in addition to the effects of *IGF2* overexpression, a decreased level of the maternally expressed gene *CDKN1C* may contribute to the BWS phenotype^{9,12,20}.

It has been demonstrated that BWS patients with paternal UPD always show mosaicism, suggesting that all cases had arisen as a postzygotic event^{19,21,22}; a possible explanation is that lack of one or more chromosome 11 maternally expressed genes may lead to embryonic lethality²³. It was also suggested that the degree of mosaicism and the location of the genetic abnormality in different tissue is strongly associated with the pathological phenotype²⁴. The extent of pUPD at chromosome 11p has been studied by means of STR markers; the critical region for pUPD is telomeric to chromosome 11p13 and always includes the region where map some BWS genes (*IGF2*, *H19* and *CDKN1C*)^{19,21,23}. Some cases with mosaic pUPD for the whole chromosome 11 have been also described and the clinical findings did not differ from patients with pUPD restricted to a small part of 11p^{23,25}. While the extent of segmental disomy and proportion of cells with pUPD is variable, in all BWS cases the paternal UPD is isodisomic. This suggests that cells with paternal UPD of chromosome 11 may have a selective growth advantage and that maternal UPD cells die or there is a partition to different parts of the conceptus²⁶.

Clinically, a clear association between mosaic UPD and hemihyperplasia exists^{15,19,22,27}. In addition, it was noted that neoplasias and Wilms' tumors are more frequent in BWS patients with pUPD or H19DMR hypermethylation than in BWS patients with other molecular defect²⁷⁻²⁹. Moreover, it has been hypothesized that extremely high levels of UPD might drive severe phenotypic expression of BWS³⁰; but it is often difficult to determine if levels of UPD correlate with severity of the phenotype especially when the tissues/organs involved are not usually directly tested. Finally, in view of the evidence of imprinted transcripts at the Wilms' tumour suppressor gene (*WT1* at 11p13)³¹⁻³³, it is interesting to evaluate whether disomy extended to *WT1* influenced the risk of neoplasia (Figure 1a).

In this paper, we evaluated a series of 9 patients with BWS due to patUPD11p using several methods with the aim to evaluate the percentage of mosaicism, the methylation status at both loci, the extent of the pUPD at the short arm and their breakpoints. Fine mapping of mitotic recombination breakpoints by SNP-array in UPD and fine estimation of epigenetic defects will provide a basis for understanding the aetiology of BWS. In addition, it would allow more accurate prognostic predictions providing a better management and surveillance of BWS children.

PATIENTS AND METHODS

Patients

From a total of 132 patients with presumptive diagnosis of BWS included in the Spanish Overgrowth Syndrome Registry, 92 had confirmed molecular diagnosis of the disorder. Among these patients we detected 71 with hypomethylation at KvDMR, 8 with point mutation on *CDKN1C* gene, 2 with hipermethylation of H19DMR and 2 with paternal duplication of 11p15.5 region. Finally, nine out of these 92 patients had laboratory results indicative of pUPD11. Clinical data of BWS individuals including personal and family history, clinical, laboratory and X-rays, pedigree, and follow-up evolution were included in a database. Parental data were also recorded. The Institutional IRB at Hospital Universitario La Paz approved this study as part of the research study at the Spanish Overgrowth Syndrome Registry (# HULP-PI446).

Cytogenetics and DNA extraction

Karyotypes were performed by standard methods in all patients. A minimum of 20 cells were counted with a resolution of at least 550 bands. FISH analysis using the D11S2071 probe was applied to all patients. DNA was extracted from blood using Qiagen kits Puregene Blood Core Kit (Maryland, USA) in all patients and available parents.

STRs segregation analyses

A panel of 6 microsatellites mapping to the short arm of chromosome 11 was evaluated in patients and their parents (when available) (Figure 1b). We used the following STRs: TH01, D11S1318, D11S4088, D11S1338, D11S1346 and D11S4046. Sequences of the primers were obtained from the NCBI public database (<http://www.ncbi.nlm.nih.gov/sites/entrez>). We calculated the percentage of mosaicism as recommended by Sasaki et al.³⁴. The calculation was as follows: $(K-1)/(K+1) \times 100$; where K is the ratio of the intensity of the parental alleles (paternal/maternal ratio) of the test sample.

Methylation-Specific MLPA (MS-MLPA)

MS-MLPA with 100 ng of genomic DNA, the SALSA ME030-B1 (11p15 region, BWS/SRS; MRC-Holland, Amsterdam, Holland) and the methylation-sensitive restriction enzyme *HhaI* (Promega Corporation) was performed according to the manufacturer's recommendations. MS-MLPA PCR products were analyzed on an ABI 3130 automated sequencer (Applied Biosystems, Foster City, California, USA). To calculate the gene dosage, the analysis of results was based on the comparison between the signals of undigested samples and undigested controls. Calculation of the methylation level of probes containing the *HhaI* restriction site was performed comparing the signals of restriction digested samples with undigested samples. The analysis of raw data was carried out using an Excel-based in-house program (Meth-HULP v1.1; available upon request). We normalized the raw value of peak areas in both controls and patient samples for undigested and digested samples and quantified gene dosage and methylation level for each sample.

Sodium bisulphite conversion and Methylation Specific-High Resolution Melting analysis (MS-HRMA)

Before MS-HRM assay, genomic DNA of controls and patients were treated with sodium bisulphite using the EZ DNA methylation Kit (Zymo research, Orange, CA, USA) according to the manufacturer's instructions. Bisulphite converts unmethylated cytosines to uracil, whereas methylated cytosines remain unreactive.

Specific primers (available upon request) to amplify H19 and KvDMR from bisulphite-converted DNA were designed by means of Methylation Primer Express Software v1.0 (Applied Biosystems). The primers amplify both methylated and unmethylated template, according to the principles set out to compensate for PCR bias³⁵. Specificity of primers was confirmed by sequencing of the PCR products. PCR amplification and MS-HRM analysis were done in a LyghtCycler 480 Real-Time PCR System (Roche Diagnostics, Germany). Normalisation of the melting curves was carried out using the software provided with the LyghtCycler 480 (Gene Scanning software v1.5). To visually estimate the curves, we included two synthetic DNA with standard methylation of 0% and 100% as controls (EpiTect PCR Control DNA Set, Qiagen). We calculated the level of methylation by the MS-HRM assay, evaluating the area under the curve in the plateau phase. The position of the plateau at the vertical scale represents the ratio between the methylated and unmethylated allele.

Pyrosequencing of imprinted centres at 11p15

Quantitative analysis of methylation at the KvDMR and H19 imprinting centres was also performed by pyrosequencing. Specific primers (available upon request) to amplify and to pyrosequence the two amplicons were designed by means of Pyrosequencing Assay Design Software (Biotage, Charlottesville, VA). The forward primer for H19 and reverse primers for KvDMR amplification were 5'-biotinylated to facilitate single-strand DNA template isolation for the pyrosequencing reaction. Preparation of the single-strand DNA template for pyrosequencing was performed using

the PSQ Vacuum Prep tool (Biotage, Charlottesville, VA) according to the manufacturer's instruction. The biotinylated PCR product was immobilized on streptavidin-coated Sepharose high-performance beads (Amersham Biosciences, Piscataway, NJ) and processed to obtain single strand DNA using the PSQ 96 Sample Preparation Kit (Biotage) according to the manufacturer's instructions. The sequencing-by-synthesis reaction of the complementary strand was automatically performed on a PSW 96MA instrument (Biotage) at room temperature using PyroGold reagents (Biotage). As nucleotides were dispensed, a light signal was generated proportional to the amount of each incorporated nucleotide. These light signals were detected by a charge-coupled device camera and converted to peaks in a sequencing program that was automatically generated in real time for each sample. The Pyro Q-CpG software (Biotage) automatically determines individual methylation frequencies for all CpG sites in the amplicon; the degree of methylation is calculated from the ratio of the peak heights of C and T.

High Density Single Nucleotide Polymorphism-arrays (SNP-arrays)

DNAs were extracted by routine methods and were quantified using PicoGreen (Invitrogen Corporation, Carlsbad, CA). A genome-wide scan of 620,901 tag SNPs was conducted on the patients, using the Illumina Human610-Quad BeadChip according to the manufacturer's specifications (Illumina, San Diego, CA). GenCall scores < 0.15 at any locus were considered "no calls". Image data was analyzed using the Chromosome Viewer tool contained in Beadstudio 3.2 (Illumina, San Diego, CA). The metric used was the log R ratio which is the log (base 2) ratio of the observed normalized R value for a SNP divided by the expected normalized R value³⁶. In addition, an allele frequency analysis was applied for all SNPs. All genomic positions were based upon NCBI Build 36 (dbSNP version 126).

RESULTS

Paternal UPD and establishment of mosaicism percentage

All 9 cases of UPD have been diagnosed by analysis of STRs markers mapping at the short arm of chromosome 11, and have shown paternal isodisomy (Supplementary Figure 1). We calculated the percentage of mosaicism by means of STRs and SNP-arrays (Figure 2a). The calculation of mosaicism using STRs has been done as recommended by Sasaki et al.³⁴ (Table Ia). Taking into account that isodisomy is paternal we could estimate the percentage of mosaicism in the SNP-array as the higher allele B frequency (Table II).

Correlation between the percentage of the UPD cells and the methylation index

As expected, the degree of mosaicism, calculated by SNP-array, and the level of methylation defect, estimated by pyrosequencing (Table Id), showed very high and statistically significant correlation: $R^2=+0.933$ for H19DMR and $R^2=-0.833$ for KvDMR (Figure 3a; Supplementary Table I).

Extent of the pUPD and correlation with methylation index and mosaicism

Fine mapping of mitotic recombination breakpoint in pUPD of chromosome 11 has been performed by SNP-array (Figure 2a, 2b). To estimate the extent of pUPD we mapped the latest SNP in pUPD and the first SNP in heterozygosis and we evaluated the minimum and the maximum size of pUPD region for each patient (Table II). We calculated the methylation index in both imprinting centres of 11p15.5 region, H19 and KvDMR, through MS-MLPA, MS-HRM and pyrosequencing analyses (Supplementary Figure 1b, 2a, 2b; Table Ib, Ic, Id). We also performed a correlation analysis between the extent of the pUPD and the level of methylation (obtained by CpG Q-Pyro) and mosaicism (calculated by STR analysis). As we expected, there has been no correlation among these parameters (Figure 3b; Supplementary Table I).

Fine mapping of the breakpoints

Fine mapping of mitotic recombination breakpoints in pUPD of chromosome 11 by SNP-arrays did not provide strong evidence for recombination hot-spots. The locations of mitotic breakpoints were different in all patients (Figure 2b; Table II). However, despite of variability of the extent of isodisomy, the region of paternal UPD invariably includes the whole imprinted gene cluster at 11p15.5 (Figure 2b).

DISCUSSION

Paternal UPD of chromosome 11p is a relatively common and cancer prone mechanism in BWS patients ²⁷ ; thus patients with this molecular subtype should be closely evaluated and prospectively followed-up. Regional or partial UPD are either caused by abnormal recombination between non-sister chromatids during mitosis or by deletion of a region and further duplication of the homologous region of the other chromosome.

From a total of 92 patients with confirmed molecular diagnosis of BWS only 9 patients (10%) had patUPD11p. This proportion is slightly lower than previous reports where close to 15-20% of the patients with BWS showed patUPD11p. This lower proportion may be due to the specific characteristics of our Registry with a high number of pregnancies obtained after assisted reproductive technologies, a procedure that it is hypothesized that predisposes to aberrant methylation of the centromeric imprinting center (IC2) ³⁷ .

Percentage of 11p mosaicism and BWS phenotype

It has been demonstrated that phenotypic expression of BWS correlates with elevated levels of UPD in the organs and tissues that were tested ²⁴ . However, it must be noted that the level of UPD has not been found to correlate with phenotypic expression. Our patients had clinical heterogeneity and lack of correlation with the percentage of mosaicism as well as the extension onto the short arm of chromosome

11. The only constant finding in all patients with patUPD11p in our series is hemihypertrophy. As an example of such lack of correlation, patient UPD 8 showed macrosomia at birth, hemihypertrophy and mild macroglossia and had 31 Mb of extension and 70 % of mosaicism and patient UPD 6 who has a smaller extension (6.6 Mb) and 64 % of mosaicism showed a more expanded phenotype including macrosomia, polyhydramnios, umbilical hernia, hemihypertrophy, macroglossia and hypoglycaemia (Supplementary Table II). Thus, larger size of mosaic UPD and/or higher percentage of mosaicism do not directly imply a more florid manifestation of the disorder. This could be due to the fact that routine testing of a single tissue, such as blood, may not actually reflect the level of UPD in the tissues most susceptible to overgrowth in BWS³⁰.

Comparison of mitotic and meiotic recombination breakpoints at 11p

Postfertilization errors such as nondisjunction with reduplication, mitotic recombination, or gene conversion might lead to complete or partial isodisomy. Mosaicism might be frequent with postfertilization errors, since there would be no selection against the original disomic line. The site of breakpoints were different in all patients suggesting that in contrast to some common breakpoints observed in meiosis there seem to be no common mitotic recombination regions^{23,38} (Table II).

Correlation of the tests

We found that a combination of two tests (MS-MLPA + MS-HRMA or MS-MLPA + pyrosequencing) is the most useful approach for clinical diagnosis. SNP-arrays alone has been useful for diagnosing UPD11p, however it cannot discriminate between paternal and maternal contribution. The costs of the studies are also important since the SNP-arrays are still expensive and should be set up in experienced laboratories. The limitations of our study are that only 9 patients were evaluated and only one tissue (blood) has been tested in these patients. In contrast, we applied five different

techniques to approach patUPD11p, including high density SNP-arrays, which in fact it would have been useful itself to solve most of the issues because it can interrogate not only the dosage but also can demonstrate the percentage of mosaicism and its extent through the short arm of chromosome 11.

Summing up, SNP-arrays have been useful and very informative for clinical diagnosis in patients with BWS with mosaic UPD11p and might be used as the unique tool in clinical diagnostic laboratories, not only to evaluate mosaicism but also to map the mitotic site and consequently the extent of UPD at the short arm of chromosome 11.

References

1. Beckwith JB Extreme cytomegaly of the adrenal fetal cortex, omphalocele, hyperplasia of kidneys and pancreas, and Leydig-cell hyperplasia: Another syndrome? Western Society for Pediatric Research 1963;
2. Elliott M, Maher ER Beckwith-Wiedemann syndrome. *J Med Genet* 1994;31:560-564.
3. Martinez RMY Clinical features in the Wiedemann-Beckwith syndrome. *Clin Genet* 1996;50:272-274.
4. Wiedemann H-R Familial malformation complex with umbilical hernia and macroglossia: A "new syndrome"? *J Genet Hum* 1964;13:223-232.
5. Maher ER, Reik W Beckwith-Wiedemann syndrome: imprinting in clusters revisited. *J Clin Invest* 2000;105:247-252.
6. Niemitz EL, DeBaun MR, Fallon J et al. Microdeletion of LIT1 in familial Beckwith-Wiedemann syndrome. *Am J Hum Genet* 2004;75:844-849.
7. Riccio A, Sparago A, Verde G et al. Inherited and Sporadic Epimutations at the IGF2-H19 locus in Beckwith-Wiedemann syndrome and Wilms' tumor. *Endocr Dev* 2009;14:1-9.
8. Lam WW, Hatada I, Ohishi S et al. Analysis of germline CDKN1C (p57KIP2) mutations in familial and sporadic Beckwith-Wiedemann syndrome (BWS) provides a novel genotype-phenotype correlation. *J Med Genet* 1999;36:518-523.
9. Lee MP, DeBaun M, Randhawa G, Reichard BA, Elledge SJ, Feinberg AP Low frequency of p57KIP2 mutation in Beckwith-Wiedemann syndrome. *Am J Hum Genet* 1997;61:304-309.

10. Romanelli V, Belinchon A, Campos-Barros A et al. CDKN1C mutations in HELLP/preeclamptic mothers of Beckwith-Wiedemann Syndrome (BWS) patients. *Placenta* 2009;30:551-554.
11. Romanelli V, Belinchon A, Benito-Sanz S et al. CDKN1C (p57(Kip2)) analysis in Beckwith-Wiedemann syndrome (BWS) patients: Genotype-phenotype correlations, novel mutations, and polymorphisms. *Am J Med Genet A* 2010;152A:1390-1397.
12. O'Keefe D, Dao D, Zhao L et al. Coding mutations in p57KIP2 are present in some cases of Beckwith-Wiedemann syndrome but are rare or absent in Wilms tumors. *Am J Hum Genet* 1997;61:295-303.
13. Reik W, Brown KW, Slatter RE, Sartori P, Elliott M, Maher ER Allelic methylation of H19 and IGF2 in the Beckwith-Wiedemann syndrome. *Hum Mol Genet* 1994;3:1297-1301.
14. Schneid H, Seurin D, Vazquez MP, Gourmelen M, Cabrol S, Le Bouc Y Parental allele specific methylation of the human insulin-like growth factor II gene and Beckwith-Wiedemann syndrome. *J Med Genet* 1993;30:353-362.
15. Engel JR, Smallwood A, Harper A et al. Epigenotype-phenotype correlations in Beckwith-Wiedemann syndrome. *J Med Genet* 2000;37:921-926.
16. Lee MP, DeBaun MR, Mitsuya K et al. Loss of imprinting of a paternally expressed transcript, with antisense orientation to KVLQT1, occurs frequently in Beckwith-Wiedemann syndrome and is independent of insulin-like growth factor II imprinting. *Proc Natl Acad Sci U S A* 1999;96:5203-5208.
17. Smilnich NJ, Day CD, Fitzpatrick GV et al. A maternally methylated CpG island in KvLQT1 is associated with an antisense paternal transcript and loss of imprinting in Beckwith-Wiedemann syndrome. *Proc Natl Acad Sci U S A* 1999;96:8064-8069.

18. Henry I, Bonaiti-Pellie C, Chehensse V et al. Uniparental paternal disomy in a genetic cancer-predisposing syndrome. *Nature* 1991;351:665-667.
19. Slatter RE, Elliott M, Welham K et al. Mosaic uniparental disomy in Beckwith-Wiedemann syndrome. *J Med Genet* 1994;31:749-753.
20. Hatada I, Ohashi H, Fukushima Y et al. An imprinted gene p57KIP2 is mutated in Beckwith-Wiedemann syndrome. *Nat Genet* 1996;14:171-173.
21. Catchpoole D, Lam WW, Valler D et al. Epigenetic modification and uniparental inheritance of H19 in Beckwith-Wiedemann syndrome. *J Med Genet* 1997;34:353-359.
22. Henry I, Puech A, Riesewijk A et al. Somatic mosaicism for partial paternal isodisomy in Wiedemann-Beckwith syndrome: a post-fertilization event. *Eur J Hum Genet* 1993;1:19-29.
23. Cooper WN, Curley R, Macdonald F, Maher ER Mitotic recombination and uniparental disomy in Beckwith-Wiedemann syndrome. *Genomics* 2007;89:613-617.
24. Itoh N, Becroft DM, Reeve AE, Morison IM Proportion of cells with paternal 11p15 uniparental disomy correlates with organ enlargement in Wiedemann-beckwith syndrome. *Am J Med Genet* 2000;92:111-116.
25. Dutly F, Baumer A, Kayserili H et al. Seven cases of Wiedmann-Beckwith syndrome, including the first reported case of mosaic paternal isodisomy along the whole chromosome 11. *Am J Med Genet* 1998;79:347-353.
26. Bischoff FZ, Feldman GL, McCaskill C, Subramanian S, Hughes MR, Shaffer LG Single cell analysis demonstrating somatic mosaicism involving 11p in a patient with paternal isodisomy and Beckwith-Wiedemann syndrome. *Hum Mol Genet* 1995;4:395-399.

27. Cooper WN, Luharia A, Evans GA et al. Molecular subtypes and phenotypic expression of Beckwith-Wiedemann syndrome. *Eur J Hum Genet* 2005;13:1025-1032.
28. Blik J, Maas SM, Ruijter JM et al. Increased tumour risk for BWS patients correlates with aberrant H19 and not KCNQ1OT1 methylation: occurrence of KCNQ1OT1 hypomethylation in familial cases of BWS. *Hum Mol Genet* 2001;10:467-476.
29. DeBaun MR, Niemitz EL, McNeil DE, Brandenburg SA, Lee MP, Feinberg AP Epigenetic alterations of H19 and LIT1 distinguish patients with Beckwith-Wiedemann syndrome with cancer and birth defects. *Am J Hum Genet* 2002;70:604-611.
30. Smith AC, Shuman C, Chitayat D et al. Severe presentation of Beckwith-Wiedemann syndrome associated with high levels of constitutional paternal uniparental disomy for chromosome 11p15. *Am J Med Genet A* 2007;143A:3010-3015.
31. Malik K, Salpekar A, Hancock A et al. Identification of differential methylation of the WT1 antisense regulatory region and relaxation of imprinting in Wilms' tumor. *Cancer Res* 2000;60:2356-2360.
32. Malik KT, Wallace JI, Ivins SM, Brown KW Identification of an antisense WT1 promoter in intron 1: implications for WT1 gene regulation. *Oncogene* 1995;11:1589-1595.
33. Ward A, Dutton JR Regulation of the Wilms' tumour suppressor (WT1) gene by an antisense RNA: a link with genomic imprinting? *J Pathol* 1998;185:342-344.
34. Sasaki K, Soejima H, Higashimoto K et al. Japanese and North American/European patients with Beckwith-Wiedemann syndrome have different frequencies of some epigenetic and genetic alterations. *Eur J Hum Genet* 2007;15:1205-1210.

35. Wojdacz TK, Hansen LL Reversal of PCR bias for improved sensitivity of the DNA methylation melting curve assay. *Biotechniques* 2006;41:274, 276, 278-
36. Simon-Sanchez J, Scholz S, Fung HC et al. Genome-wide SNP assay reveals structural genomic variation, extended homozygosity and cell-line induced alterations in normal individuals. *Hum Mol Genet* 2007;16:1-14.
37. Amor DJ, Halliday J A review of known imprinting syndromes and their association with assisted reproduction technologies. *Hum Reprod* 2008;23:2826-2834.
38. Russo S, Finelli P, Recalcati MP et al. Molecular and genomic characterisation of cryptic chromosomal alterations leading to paternal duplication of the 11p15.5 Beckwith-Wiedemann region. *J Med Genet* 2006;43:e39-

ACKNOWLEDGMENTS:

Grant sponsor: Fondo de Investigación Sanitaria (FIS); Grant number: PI08/1360.

Titles and legends to figures

Figure 1. (a) Schematic view of chromosome 11. Zoom of a part of 11p showing the location of genes and imprinting centres of 11p15.5 BWS locus and *WT1* gen. (b) Location of the 6 STR markers evaluated in patients and their parents.

Figure 2. (a) SNP-array results for two UPD patients (UPD 4 and UPD 7). The B allele frequency is shown in the upper panel of each patient. The red zone represents the chromosome fragment with UPD and the level of mosaicism for each SNP. The graph Log R Ratio is the measure of genomic dosage (normal in both patients). Note the differences presented by these two cases on the extent of UPD fragment and their level of mosaicism which is higher for patient UPD 4 than UPD 7. (b) Graphic representation of the UPD extension for each patients and the latest SNP involved in the breakpoint.

Figure 3. Scatter graph of Spearman's correlations and relatives R^2 values. (a) These two graphs represent the direct and inverse correlation between the percentage of mosaicism and the methylation level at H19DMR and KvDMR loci respectively. (b) Graphic representation showing that there is no correlation between the size of the UPD fragment and the methylation level of both imprinting centres and the percentage of mosaicism.

Supplementary Figure 1. (a) Example of microsatellite analysis; patient, mother and father are represented from top to bottom. Note the paternal origin of UPD and the different level of mosaicism denoted from the different contribution of paternal and

maternal alleles in patients' results. (b) Methylation analysis by MS-MLPA in two representative patients. Note the different extent of epigenetic defect compared to controls' mean methylation. To higher level of mosaicism corresponds to higher hypermethylation of H19DMR and increased hypomethylation of KvDMR (and vice versa).

Supplementary Figure 2. (a) MS-HRM results of two patients (UPD 1 and UPD 7). In the first and in the second panel H19DMR and KvDMR curves are represented respectively. Note the different level of methylation between both patients; controls' DNA (C), 0% and 100% methylated synthetic DNAs are used to visually appreciate the curve variation. (b) Pyrosequencing image of the three first dinucleotidos CpG for H19DMR and KvDMR in patients UPD 1 and UPD 7. Results of the methylation percentage for each CpG individually are similar to the MS-HRM results.

Table I. Estimated percentage of cells with UPD calculated for each STR markers (a); methylation index calculated by MS-MLPA (b), MS-HRM (c) and pyrosequencing (d) for each patient. For the methylation analysis it has been calculated the normal methylation index as controls' mean value and standard deviation, for each technique.

a						
Patient	STR markers					
	D11S4046	D11S1318	D11S4088	D11S1338	D11S1346	TH01
UPD 1	85,77%	82,01%	77,77%	53,49%	-	89,38%
UPD 2	16,82%	47,91%	31,82%	48,47%	50,52%	37,52%
UPD 3	-	57,44%	21,49%	-	51,23%	41,39%
UPD 4	74,14%	73,08%	73,62%	51,26%	67,87%	64,08%
UPD 5	33,35%	45,58%	40,59%	-	74,83%	63,51%
UPD 6	81,70%	66,48%	31,26%	-	9,07%	36,31%
UPD 7	12,93%	28,35%	32,39%	22,79%	-	-
UPD 8	50,19%	-	63,11%	50,46%	53,73%	49,17%
UPD 9	58,78%	38,82%	73,84%	37,68%	45,54%	-

Patient	b		c		d	
	MS-MLPA		MS-HRM		CpG Q-Pyro	
	H19DMR 1	KvDMR	H19DMR	KvDMR	H19DMR	KvDMR
UPD 1	114,77%	8,89%	60,98%	24,19%	90,61%	10,96%
UPD 2	81,25%	31,70%	46,01%	48,91%	73,15%	27,94%
UPD 3	59,81%	42,76%	46,17%	53,24%	64,80%	28,31%
UPD 4	79,99%	21,38%	50,41%	40,36%	86,78%	20,50%
UPD 5	73,47%	23,22%	50,84%	36,46%	79,22%	18,59%
UPD 6	69,27%	33,98%	51,99%	50,68%	72,07%	26,05%
UPD 7	70,32%	42,05%	44,37%	48,52%	67,75%	29,13%
UPD 8	69,09%	34,47%	52,41%	45,96%	74,26%	28,34%
UPD 9	86,18%	35,85%	51,89%	50,48%	73,26%	22,99%

Controls' mean	50,26%	54,69%	39,64%	59,67%	52,11%	40,68%
Std. Desv.	7,18%	4,63%	2,07%	3,74%	2,02%	5,17%

Table II. SNP-array analyses results. The minimum and maximum size estimated for the UPD extent and the gap between these two values are shown. The breakpoints were estimated by means of the identification of the last SNP affected by UPD and the first SNP in heterozygosis. The lower and higher B allele frequencies for all SNPs were calculated. Taking into account that isodisomy is paternal, the percentage of mosaicism of UPD cells is considered to be represented by the frequency of superior B allele.

Patient	Latest UPD SNP	Position	First Het SNP	Position	Min UPD Size (Mbp)	Gap (Kbp)	Max UPD Size (Mbp)	Inferior B Allele Freq	Superior B Allele Freq	Stand dev
UPD 1	rs10838427	45,138,258	rs11038507	45,495,455	45,138	357,197	45,495	10,5%	89,5%	4,8%
UPD 2	rs10838591	46,230,719	rs8914	46,655,700	46,231	424,981	46,656	31,6%	68,4%	4,2%
UPD 3	rs35834377	41,774,946	rs11036703	42,105,122	41,775	330,176	42,105	35,5%	64,5%	4,2%
UPD 4	rs11038116	44,680,447	rs704664	44,743,777	44,681	63,330	44,744	23,1%	76,9%	4,6%
UPD 5	rs1061022	32,083,259	rs7105777	32,997,914	32,083	914,655	32,998	23,1%	76,9%	4,3%
UPD 6	rs2063082	6,624,904	rs11040978	6,690,629	6,625	65,725	6,691	35,7%	64,3%	6,5%
UPD 7	rs10832514	2,645,102	rs151288	2,742,878	2,645	97,776	2,743	39,1%	60,9%	3,3%
UPD 8	rs2177482	31,758,933	rs11031505	31,855,115	31,759	96,182	31,855	30,0%	70,0%	3,5%
UPD 9	rs2288249	46,290,815	rs876701	46,327,343	46,291	36,528	46,327	29,4%	70,6%	3,7%

Supplementary Table I. Spearman's rank correlation coefficient (or Spearman's rho) is a non-parametric measure of statistical dependence between two variables. It assesses how well the relationship between two variables can be described using a monotonic function. In the ovals the correlation coefficients and the statistical significant of the correlation are highlighted. In the vertical ovals there is no correlation between the size of UPD fragment, the percentage of methylation at both imprinting centres and the level of mosaicism. In the horizontal oval are shown a direct correlation between the level of mosaicism and the percentage of methylation of H19DMR ($r=+0.933$) and an inverse correlation ($r=-0.833$) between the level of mosaicism and the percentage of methylation of KvDMR; both correlations are statistically significant.

Correlations

			IC I (H19KvDMR)/CpG Q-Pyro	IC II (KvDMR)/CpG Q-Pyro	Sup B Allele Freq	Min UPD Size (Mbp)
Spearman's rho	IC I (H19KvDMR)/CpG Q-Pyro	Correlation Coefficient	1.000	-.767*	.933**	.367
		Sig. (2-tailed)	.	.016	.000	.332
		N	9	9	9	9
	IC II (KvDMR)/CpG Q-Pyro	Correlation Coefficient	-.767*	1.000	-.833**	-.500
		Sig. (2-tailed)	.016	.	.005	.170
		N	9	9	9	9
	Sup B Allele Freq	Correlation Coefficient	.933**	-.833**	1.000	.583
		Sig. (2-tailed)	.000	.005	.	.099
		N	9	9	9	9
	Min UPD Size (Mbp)	Correlation Coefficient	.367	-.500	.583	1.000
		Sig. (2-tailed)	.332	.170	.099	.
		N	9	9	9	9

*. Correlation is significant at the .05 level (2-tailed).

**. Correlation is significant at the .01 level (2-tailed).

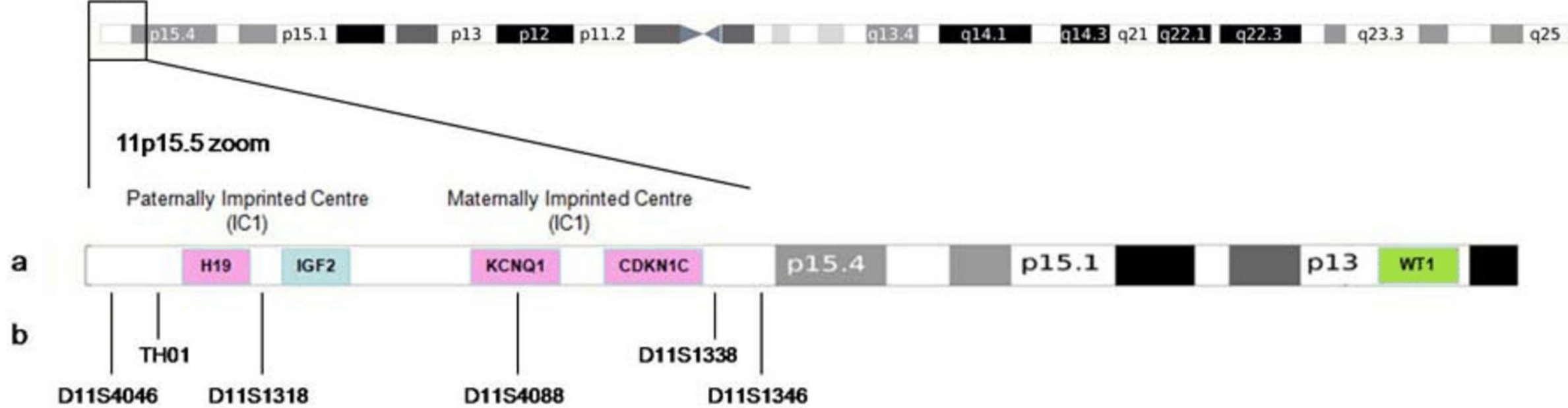
Supplementary Table II. (a) Molecular results and clinical findings of each patient. (b) Summary table with frequency of main clinical signs in our of patients.

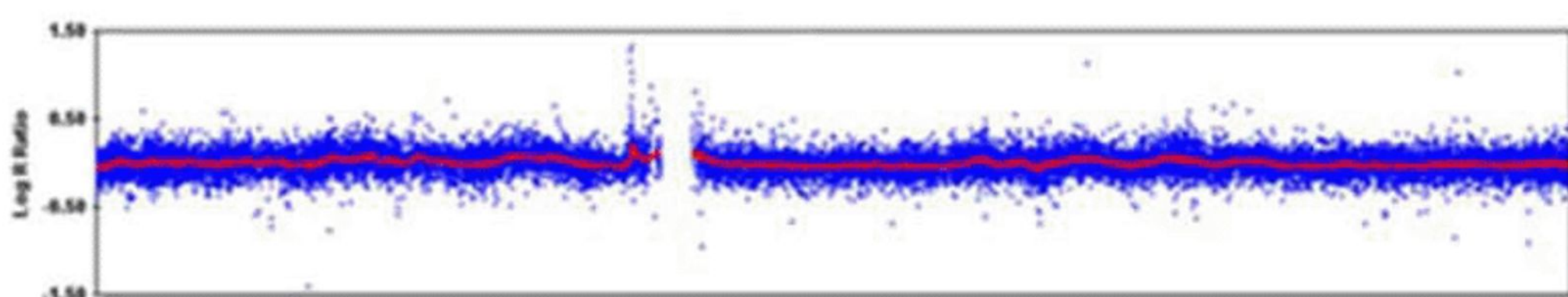
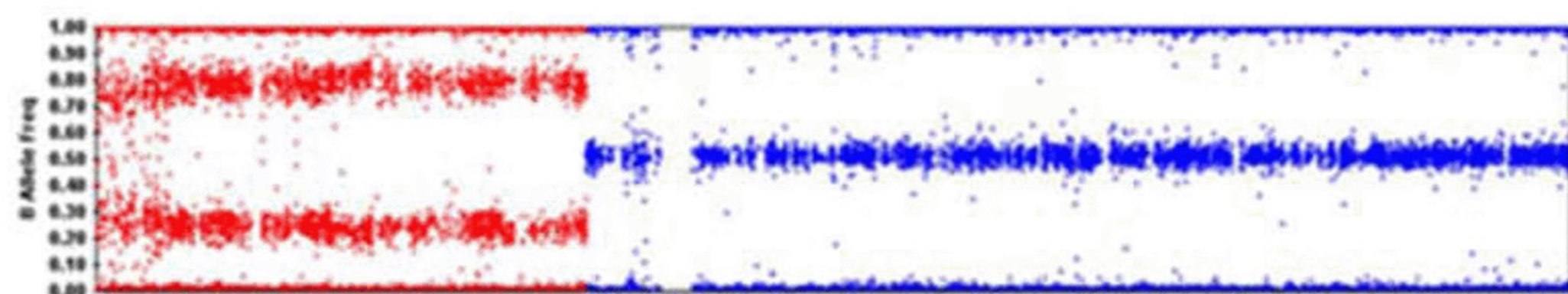
a

Patient	UPD 1	UPD 2	UPD 3	UPD 4	UPD 5	UPD 6	UPD 7	UPD 8	UPD 9
Sex	Male	Male	Female	Female	Male	Male	Female	Male	Male
Age at diagnosis	3y 11m	4y 5m	2y 3m	2y 4m	2y 4m	1y 5m	2y 1m	3m	5m
% of mosaicism	89,5%	68,4%	64,5%	76,9%	76,9%	64,3%	60,9%	70,0%	70,6%
UPD extent	45,1Mbp	46,2Mbp	41,8Mbp	44,7Mbp	32,1Mbp	6,6Mbp	2,6Mbp	31,7Mbp	46,3Mbp
Pregnancy	Polyhydramnios	Polyhydramnios	-	-	-	Polyhydramnios	-	-	Polyhydramnios
Birth weight (g)	Increased (... g)	Increased (... g)	Increased (... g)	Increased (... g)	Increased (... g)	Increased (... g)	Increased (... g)	Increased (... g)	Increased (... g)
Hemihyperplasia	Hemihyperplasia	Left hemihyperplasia	Right hemihyperplasia	Right hemihyperplasia	Left hemihyperplasia	Hemihyperplasia	Right hemihyperplasia	Right hemihyperplasia	Hemihyperplasia
Craneofacial	Macroglossia; ear creases	Macroglossia	-	-	Macroglossia; ear creases	Macroglossia	Macroglossia	-	Macroglossia; ear creases
Cardiovascular	-	-	-	Atrial septal defect	-	-	-	-	-
Abdomen	Omphalocele	Umbilical hernia	Omphalocele	-	-	Umbilical hernia	-	-	Umbilical hernia
Skin	Capillary malformation	Capillary malformation	-	-	-	-	-	-	Capillary malformation
Wilms' tumor	-	-	-	-	-	-	-	-	-
Others	Hypoglycaemia	Hypoglycaemia	Hypoglycaemia	Pulmonary stenosis	Hypoglycaemia	Hypoglycaemia	-	-	Hypoglycaemia

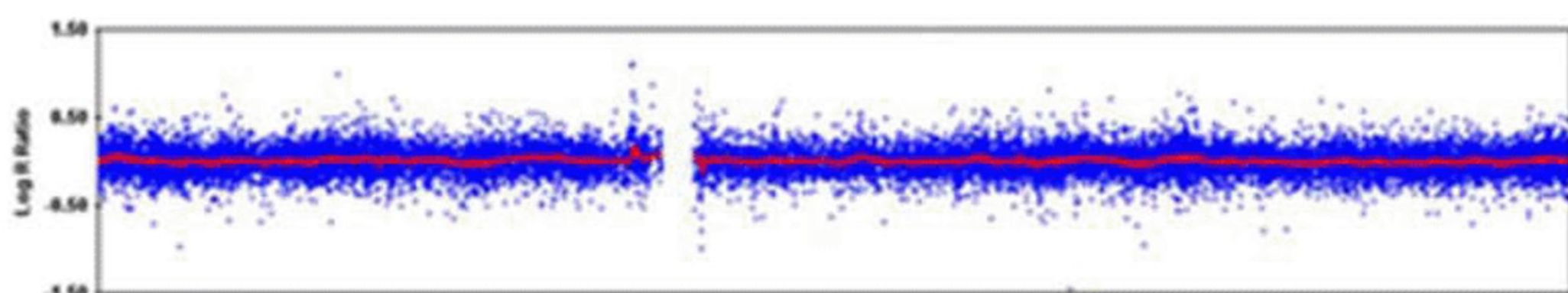
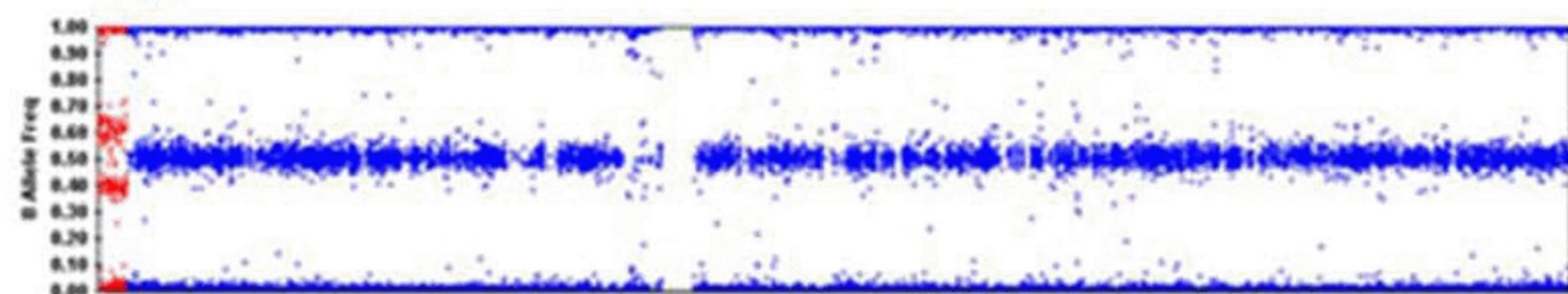
b

Clinical Findings	
Male:Female	6:3
Polyhydramnios	4/9
Increased birth weight	9/9
Hemihyperplasia	9/9
Macroglossia	6/9
Ear creases	3/9
Omphalocele	2/9
Umbilical hernia	3/9
Capillary malformation	3/9
Wilms' tumor	0/9
Hypoglycaemia	6/9



a UPD 4

UPD 7

**b** BWS locus